

Interactive Impacts of Uncertainties in Bias-Corrected Hydrologic Simulations: Southern China

Chen Li¹, Guohe Huang^{*1}, and Guanhui Cheng¹

¹University of Regina

November 23, 2022

Abstract

This study aims to comprehensively examine diverse uncertainties/multiplicities (e.g., performance indicators, bias-correction methods, hydrologic models, bias-correction schemes, predictor combinations, watersheds, streamflow magnitudes, and temporal scales) in bias-corrected hydrologic simulations (BCHS). The focus is placed on the variations of BCHS accuracies (representing climatic impacts on runoffs) with every uncertainty, as well as their interactions with the other uncertainties. To achieve this, an integrated bias-corrected hydro-modeling uncertainty analysis approach (IBCHMUA) is developed based on one advanced hydro-modeling method, i.e., discrete principal-monotonicity inference (DiPMI), and two hydrologic models, i.e., Xin'anjiang and HyMOD. IBCHMUA is applied to two representative watersheds (Xiangxi and Zhongzhou) in southern China. Many findings are revealed. For instance, it is necessary to apply multiple performance indicators and DiPMI is effective in correcting hydro-model biases. Every uncertainty poses significant impacts on BCHS, and the significance of the impacts further varies with all or part of the other uncertainties. BCHS accuracies (or the estimated climatic impacts on runoffs in southern China) increase from daily to monthly scales, from Xiangxi to Zhongzhou Watersheds, from the highest through the lowest to the overall runoff magnitudes, from Xin'anjiang to HyMOD models, and from original to bias-corrected hydrologic simulations. Meanwhile, the impacts of the uncertainties in BCHS decrease from bias-correction schemes, temporal scales, streamflow magnitudes, hydrologic models or predictor combinations, to watersheds. These findings are helpful for reducing the complexity and enhancing the reliability of BCHS under diverse uncertainties, and point out the importance of taking into account the interactions of the uncertainties in BCHS studies.

1 **Interactive Impacts of Uncertainties in Bias-Corrected Hydrologic Simulations: Southern**
2 **China**

3
4 **Chen Li¹, Guohe Huang^{1*}, Guanhui Cheng^{1*}**

5 ¹ Institute for Energy, Environment and Sustainable Communities, University of
6 Regina, Regina, Saskatchewan S4S 0A2, Canada

7 Corresponding author: Guohe Huang (huang@iseis.org); Guanhui Cheng
8 (guanhuicheng@gmail.com).

9
10 **Key Points:**

- 11 • An approach was developed to comprehensively examine diverse uncertainties
12 in bias-corrected hydrologic simulations over southern China.
- 13 • Uncertainty impacts: bias-correction schemes > temporal scales > streamflow
14 magnitudes > hydrologic models or predictor combinations > watersheds.
- 15 • Every uncertainty poses significant impacts on simulations, which further
16 varies with all or part of the other uncertainties.

17
18 **Abstract:**

19 This study aims to comprehensively examine diverse uncertainties/multiplicities
20 (e.g., performance indicators, bias-correction methods, hydrologic models, bias-
21 correction schemes, predictor combinations, watersheds, streamflow magnitudes, and
22 temporal scales) in bias-corrected hydrologic simulations (BCHS). The focus is
23 placed on the variations of BCHS accuracies (representing climatic impacts on
24 runoffs) with every uncertainty, as well as their interactions with the other
25 uncertainties. To achieve this, an integrated bias-corrected hydro-modeling
26 uncertainty analysis approach (IBCHMUA) is developed based on one advanced
27 hydro-modeling method, i.e., discrete principal-monotonicity inference (DiPMI), and
28 two hydrologic models, i.e., Xin'anjiang and HyMOD. IBCHMUA is applied to two
29 representative watersheds (Xiangxi and Zhongzhou) in southern China. Many
30 findings are revealed. For instance, it is necessary to apply multiple performance
31 indicators and DiPMI is effective in correcting hydro-model biases. Every uncertainty
32 poses significant impacts on BCHS, and the significance of the impacts further varies
33 with all or part of the other uncertainties. BCHS accuracies (or the estimated climatic
34 impacts on runoffs in southern China) increase from daily to monthly scales, from
35 Xiangxi to Zhongzhou Watersheds, from the highest through the lowest to the overall
36 runoff magnitudes, from Xin'anjiang to HyMOD models, and from original to bias-
37 corrected hydrologic simulations. Meanwhile, the impacts of the uncertainties in
38 BCHS decrease from bias-correction schemes, temporal scales, streamflow
39 magnitudes, hydrologic models or predictor combinations, to watersheds. These
40 findings are helpful for reducing the complexity and enhancing the reliability of

41 BCHS under diverse uncertainties, and point out the importance of taking into
42 account the interactions of the uncertainties in BCHS studies.

43

44 **Keywords:** hydrologic modeling, bias correction, DiPMI, uncertainty analysis, China.

45

46 **1.Introduction**

47 Hydrologic simulation is crucial for understanding hydrologic systems and
48 mitigating hydrologic risks (e.g., droughts and floods) under climatic and
49 anthropogenic impacts. Nevertheless, biases (i.e., systematic errors) exist because it is
50 challenging for hydrologic models to perfectly reproduce complex hydrologic
51 processes (Piani et al., 2010; Roberto Buizza, 2005). The biases would reduce the
52 robustness of hydrologic simulation, the reliability of the corresponding water
53 resources management schemes, and the reasonableness of socio-economic and eco-
54 environmental development (Piani et al., 2010; Saber et al., 2018). Correcting biases
55 of hydrologic simulation through effective methods is required for eliminating these
56 consequences and enhancing the sustainability and resilience of water resources
57 systems.

58 Correspondingly, bias correction was proposed. Representative methods consist
59 of linear scaling, power transformation, and quantile mapping (Shrestha et al., 2017).
60 These methods presented encouraging performances in correcting averages, variances,
61 distributions, or other features of biases in hydrologic simulation, while their
62 effectiveness was limited in some cases. Meanwhile, a series of sophisticated
63 statistical methods emerged for hydrosystem analyses and might overperform existing
64 ones in bias correction. As a representative, discrete principal-monotonicity inference
65 (DiPMI) (G. Cheng et al., 2016b, 2016a; G. H. Cheng et al., 2017) can be used to
66 enhance the reliability of hydro-model bias correction, and to reveal the joint,
67 dominant, interactive, and non-monotonic impacts of climatic conditions on
68 streamflow. Correcting biases of hydrologic simulation through both conventional and
69 emerging methods deserves exploration.

70 In addition, many multiplicities (i.e., uncertainties in most hydrologic,
71 geophysical or other relevant studies) exist and propagate in bias-corrected hydrologic
72 simulation (BCHS) (Cheng et al., 2017; Ehret et al., 2012). Typical ones include the
73 multiplicities/uncertainties of hydrologic models, bias-correction methods, predictor
74 selections, watersheds, temporal scales, streamflow magnitudes, etc. Neglecting them
75 (e.g., choosing one hydrologic model corrected by one method to represent a
76 hydrologic system of uncertain structures) would lead to arbitrary BCHS results,
77 unilateral research findings, and unreliable decision support. Examining these
78 uncertainties is conducive to enhancing the reliability of hydrologic simulation and
79 the related water resources management and engineering practices (Vetter et al.,
80 2017).

81 In this regard, many studies have been conducted. For instance, Beven et al.
82 (1992) analyzed the uncertainties of hydrologic models by the GLUE method (Beven
83 and Binley, 1992). The selection of bias-correction methods had a more significant
84 impact on runoff extremes than runoff averages (Lenderink et al., 2007). Different

85 simulation structures or conceptualizations might result in significant uncertainties in
86 hydrologic predictions (Arkesteijn and Pande, 2013). Addor et al. (2014) identified
87 the dominant impacts of uncertainties in climate models, emission scenarios, post-
88 processing methods, and catchments. However, few studies took all aforementioned
89 uncertainties into account and revealed their interactive impacts on hydro-simulation
90 reliabilities. This gap may decrease the robustness of hydrologic simulations, increase
91 the unreliability of simulation-based decision support, and hinder the mitigation of
92 hydrologic hazards (e.g., floods and droughts).

93 Therefore, the objective of this study is to develop an integrated bias-corrected
94 hydro-modeling uncertainty analysis approach (IBCHMUA) for comprehensively
95 examining interactive impacts of diverse uncertainties (especially their interactive
96 impacts) in BCHS. Specifically, Section 2 introduces two representative catchments in
97 southern China, and the necessity of this study for local water resources management.
98 Section 3 presents the principle of DiPMI and the framework of IBCHMUA. Section
99 4 focuses on the variations of BCHS performances with method-related uncertainties
100 (i.e., performance indicators, bias-correction methods, hydrologic models, bias-
101 correction schemes, and predictor combinations). Section 5 elaborates the variations
102 with non-method uncertainties (i.e., watersheds, streamflow magnitudes, and temporal
103 scales), as well as the interactions of all uncertainties. Section 6 summarizes the
104 innovation, findings, and potential extensions of this study.

105

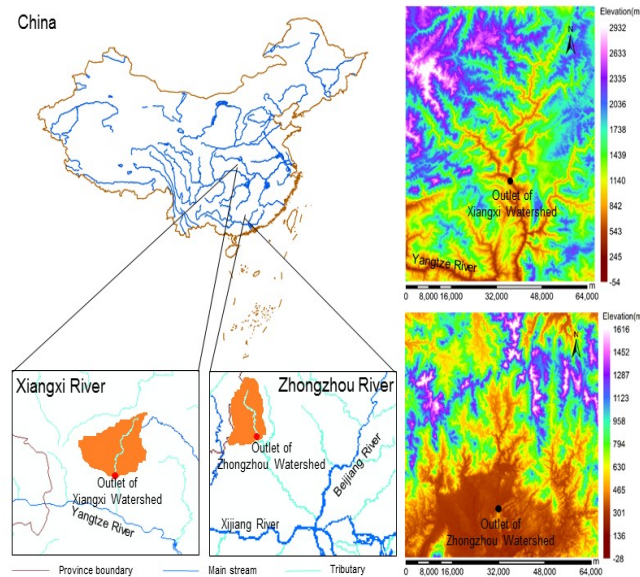
106 **2. Study Areas: Southern China**
107 **(1) Representative Watersheds**

108 Southern China is one of the most economically active areas across the world.
109 Two large rivers (i.e., Yangtze River and Pearl River) are supporting extensive socio-
110 economic activities (e.g., agriculture, fishery, shipping and industries) over this
111 region. As rapidly developing areas in economics, both river basins are the frontier of
112 scientific and technological innovation in China (Liu et al., 2018; Zhang et al., 2016).
113 In this study, two watersheds (Figure 1) are selected due to their representative
114 characteristics (as specified below) of watersheds in the river basins.

115 Xiangxi Watershed is an upstream tributary of Yangtze River that is closest to the
116 Three Gorges Dam. It is located between 30.99° N and 31.67° N and between 110.47°
117 E and 111.06° E. Its mainstream, Xiangxi River, reaches a length of 97.3 kilometers
118 and a drainage area of 1189 km². This river has two sources, i.e., Shendu River of
119 64.5 kilometers in the east, and Baisha River of 54 kilometers in the west. Both rivers
120 intersect at Gaoyang Town, Xingshan County. The elevation of the Watershed ranges
121 from 67 to 3088 meters, and the average slope is 1.42%. In contrast, Zhongzhou
122 Watershed (Figure 1) has a length of 136.5 kilometers and a drainage area of 2,328
123 km². Its mainstream, Xiaohuanjiang River, is the secondary tributary of Beijiang
124 River in Pearl River Basin. It is located between 23.96° N and 24.44° N and between
125 112.02° E and 112.26° E. Its elevation fluctuates from 61 to 1411 meters, and the
126 average slope is 0.76%.

127 In addition, both mountainous watersheds have narrow and twisted river
128 channels, and fast river flows. High coverages of forests and red soils lead to low

129 sediment concentrations in both watersheds. The forest-coverage rates of Xiangxi and
 130 Zhongzhou Watersheds are 80.02% and 72.63%, respectively. Xiangxi Watershed is
 131 full of shoals without waterway transportation, the river valley (i.e., ≤ 800 m) is
 132 composed of purple sand shales and argillaceous rocks, and the high-altitude area is
 133 dolomites, siliceous rocks and limestones. In comparison, Zhongzhou Watershed is
 134 characterized by magmatic rocks and granites, few dangerous shoals, efficient
 135 shipping conditions, and developed waterway transportation.
 136



137
 138 Figure 1. Locations and topographic characteristics of selected watersheds in
 139 Southern China.
 140

141 (2) Climatic and Hydrologic Features

142 The climatic conditions that significantly drive changes of streamflow are
 143 identified through correlation analysis. A group of data for hydrological simulation are
 144 obtained by Kriging interpolation. Based on the finalized datasets for both
 145 watersheds, hydroclimatic characteristics are primarily analyzed to facilitate
 146 subsequent bias-corrected hydrologic simulation. Critical results of the analysis are
 147 presented as follows.

148 Multi-year averages of daily discharges at outlets are $30.2 \text{ m}^3/\text{s}$ in Xiangxi
 149 Watershed and $30.5 \text{ m}^3/\text{s}$ in Zhongzhou Watershed. Annual average numbers of flood
 150 peaks ($\geq 100 \text{ m}^3/\text{s}$) are 75 and 83 for Xiangxi and Zhongzhou Watersheds,
 151 respectively. Both rivers are prone to floods in flooding seasons. Precipitation and
 152 evaporation have the highest correlation with runoffs, which are 0.89 and 0.76
 153 respectively. The driving force of the two climate conditions for runoffs is stronger
 154 than the others.

155 Both watersheds belong to subtropical monsoon climates, with flood seasons

156 from April to September, dry seasons from October to March of the next year, and no
157 frozen seasons. Zhongzhou Watershed is more susceptible to heavy precipitation in
158 summer than Xiangxi Watershed, which may be associated with high vulnerability of
159 southeastern coastal areas of China to typhoons. The annual average number of
160 precipitation days in Xiangxi Watershed is 128.8, while that in Zhongzhou Watershed
161 is 159.6. The numbers of days precipitation exceeding 50 and 100 mm in Xiangxi
162 Watershed are 9 (0.49% of total days) and 1 (0.05%), respectively; they are 36
163 (1.97%) and 8 (0.04%) for Zhongzhou Watershed, respectively. The highest
164 temperature in Xiangxi Watershed is 41.5 °C and the lowest is -4.5 °C; in Zhongzhou
165 Watershed, they are 38.7 and -0.9 °C, respectively. The numbers of days with above
166 35 °C in Xiangxi and Zhongzhou Watersheds are 40.6 and 39.8, respectively. Heavy
167 precipitation dominates streamflow changes. This indicates the existence of extreme
168 climatic events in both watersheds.

169

170 **(3) Research Necessity**

171 Both watersheds as well as many others in southern China are prone to
172 hydrologic hazards, i.e., floods, droughts and the related events (e.g., landslides,
173 mudslides, or mountain torrents). Changing climates, dense populations, and
174 prosperous economies in the watersheds aggravate socio-economic and eco-
175 environmental effects of the hazards. Particularly, both watersheds suffer from
176 varying degrees of economic losses each year. For instance, heavy precipitation
177 triggered a 50-year flood in Xiangxi Watershed on August 23, 2011. As a result,
178 streamflow overtopped river banks, flooded riverine communities, destroyed national
179 road sections, affected over 22,000 people, and caused severe economic losses. In
180 October 2004, the drought area of Zhongzhou Watershed was 7,093 hectare, including
181 3,000 hectare of serious drought areas. Meanwhile, extreme weather shows higher
182 risks and severer impacts under climate change (McBean et al., 2019).

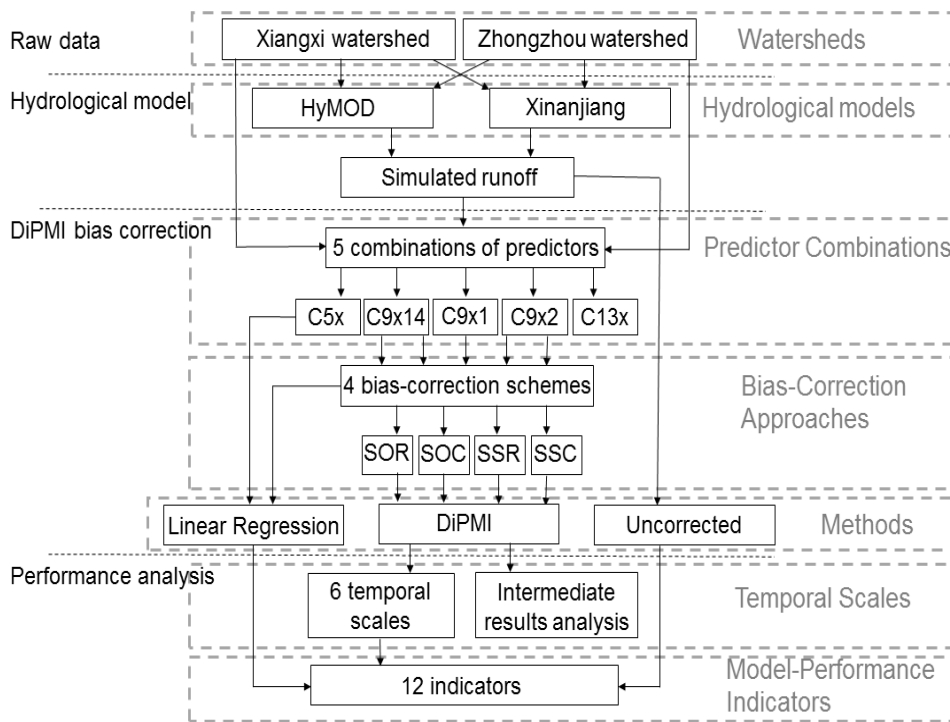
183 Reliable hydrologic forecasting is highly required for guiding strategic flood
184 control, drought mitigation, policy making, engineering practices, and public
185 engagement in addressing potential hydrologic hazards over the two watersheds under
186 climate change. This depends on the reliability of hydrologic modeling in reproducing
187 climatic impacts on historical hydrologic regimes. One challenge for this is the
188 existence of biases in hydrologic modeling, and another is diverse uncertainties (e.g.,
189 hydrologic models, bias-correction methods, and temporal scales) in correcting them.
190 Hydrologic modeling and forecasting without integrated analyses of the uncertainties
191 in bias correction is hardly reliable for providing scientific decision support, and may
192 aggravate socio-economic and eco-environmental consequences of hydrologic
193 hazards under climate change. Thus, this study focuses on the analyses of diverse
194 uncertainties (especially their interactive impacts on hydroclimatic responsive
195 relationships) in bias-corrected hydrologic simulation of Xiangxi and Zhongzhou
196 Watersheds in southern China.

197

198 **3. Methodology**

199 **(1) Research Framework**

200 An integrated approach is proposed to systematically analyze diverse
201 uncertainties in bias-corrected hydrologic simulations (especially interactive impacts
202 of uncertainties). It is named as integrated bias-corrected hydrologic modeling
203 uncertainty analysis (IBCHMUA) in this study. Its flowchart is shown in Figure 2.
204 Specifically, (i) the historical observations of runoffs and the related climatic
205 conditions are extracted through fundamental data processing; (ii) two hydrologic
206 models are employed to simulate climatic impacts on runoffs; (iii) according to five
207 predictor selection schemes, a set of datasets involving hydrologic simulations and
208 hydroclimatic observations are constructed for bias corrections; (iv) for every dataset,
209 biases in hydrologic simulation are corrected by DiPMI and other methods through
210 four different approaches (e.g., day-to-day or distributional corrections); and (v)
211 twelve indicators such as the Nash-Sutcliffe efficiency coefficient (Krause et al.,
212 2005) and the root mean square error (Ye et al., 2014) are introduced to represent the
213 multi-dimensional accuracies of all simulations.
214



215

216 Figure 2. Flowchart of IBCHMUA (all abbreviations are specified in Tables 1 and 2.

217

218 **(2) DiPMI**

219 DiPMI (i.e., discrete principal-monotonicity inference) is an advanced statistical
220 classifier for quantifying concurrent variations of dependent variables (Y) with
221 independent variables (X) through recursive classifications of X-Y samples and
222 statistical inferences of classified results. The fundamental algorithm of DiPMI is
223 mainly based on the theories of multivariate variance and discrimination analyses
224 (Cheng et al., 2016a). The algorithm is illustrated in Figure 3, and is briefly

225 introduced as follows.

226 Step 1: A normality test is conducted to analyze whether the predictand (y) (e.g.,
227 observed runoffs in this study) is normally distributed. If the test does not pass, y is
228 converted by a discrete method (Cheng et al., 2016a) to a normal distribution based on
229 the invertible transformation between the $[0, 1]$ uniform distribution and the
230 cumulative distribution of y . The distribution of y is restored by the discrete method
231 after construction of a DiPMI-based bias-correction model.

232 Step 2: Two sub-modules, i.e., classification and clustering, are employed to
233 group the variations of y with multiple predictors (X) (e.g., simulated runoffs and
234 observed climates in this study). Multi-year paired data series (X, y) are classified as a
235 series of different nodes in the former sub-module, while the latter clusters any two
236 similar nodes of (X, y). Both are recursively conducted to discretize the responsive
237 relationship between X and y as nodes (constituting a DiPMI model) (Cheng et al.,
238 2017; Cheng et al., 2017).

239 Steps 3&4: The Nash coefficient (Ye et al., 2014) is introduced to quantify model
240 accuracies. Two model parameters N_{\min} (i.e., the minimum sample size in nodes) and
241 α (i.e., the statistical significance level) are calibrated through greedy search (Steven
242 et al., n.d.) and a two-stage calibration strategy (Cheng et al., 2016a). The
243 performance of the calibrated DiPMI model is verified through another (X, y) series.

244 DiPMI was initially developed for modeling complicated hydrologic systems
245 under irregular nonlinearities, multivariate dependencies, and data uncertainties
246 (Cheng et al., 2016a). One unique advantage of this method is that it could reveal the
247 joint, dominant, interactive, and non-monotonic impacts of multiple influencing
248 factors (e.g., climatic conditions) on hydrologic variables based on rigorous statistical
249 inferences. As an emerging advanced statistical method, DiPMI may outperform
250 conventional bias-correction methods (e.g., linear regression). Thus, both methods are
251 incorporated into the framework of IBCHMUA to address the uncertainty of bias-
252 correction methods.

253

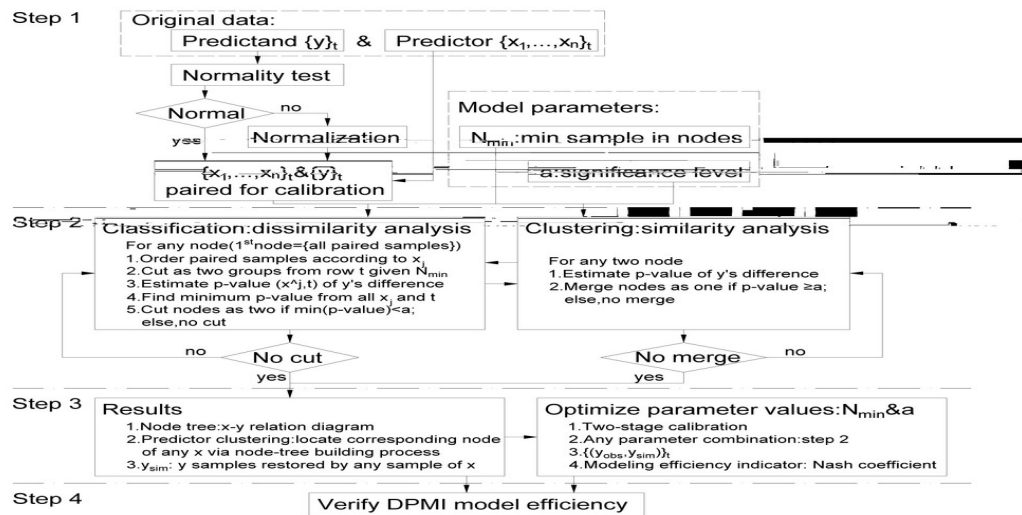


Figure 3. Procedures of discrete principal-monotonicity inference.

254

255

256

(3) Uncertainty of Hydrologic Models

258

259

260

261

262

263

264

265

266

267

268

269

270

271

272

273

274

275

276

BCHS (i.e., bias-corrected hydrologic simulation) consists of multiple modules, e.g., hydrologic modeling, bias correction, and predictor selection. For each module, multiple models, methods, approaches or options are available, and the uncertainty may pose significant impacts on BCBS results and findings. These uncertainties are named as method uncertainties to structuralize various uncertainties that are taken into account in this study. To reflect each of them, multiple options are employed in the IBCHMUA approach. These options are briefly explained as follows.

It has been reported that the uncertainty of hydrologic models has an essential contribution to hydro-simulation uncertainties. To reflect such an uncertainty, two hydrologic models (i.e., HyMOD and Xinanjiang) are calibrated through the SCEUA algorithm (Tu & Smith, 2018) to simulate runoffs at outlets of the two watersheds (i.e., Xiangxi and Zhongzhou). The HyMOD model (Yin et al., n.d.) conceptualizes runoff generation by a water storage capacity curve, and flow routing by two linear tanks. In comparison, the Xinanjiang model (Yuan et al., 2008) characterizes hydrologic processes as three modules, i.e., three-layer evapotranspiration, runoff generation, and runoff routing. Both models are suitable for southern China of humid climates and their suitability has been verified in previous studies (Liu et al., 2018; Wi et al., 2015; Zhang et al., 2016).

277 (4) Uncertainty of Bias-Correction Methods & Schemes

278 In consideration of the uncertainty of bias-correction methods, two methods (i.e.,
279 DiPMI and linear regression) are used to correct biases of the two hydrologic models.
280 Meanwhile, multiple schemes exist for any bias-correction method, and such an
281 uncertainty may also significantly influence hydrologic simulations (Chen et al.,
282 2013; Haerter et al., 2011). For instance, correction can focus on either both
283 magnitudes and timing of biases, or overall distributions; the former scheme is
284 suitable for the cases (e.g., flood control) where timing of streamflow is critical, while
285 the latter for those (e.g., engineering design) concentrating on multi-year distributions
286 of streamflow. Besides, the selection of samples for calibration and verification can be
287 either random or chronological at a given ratio (e.g., 4:1); these selections are suitable
288 for stationary and nonstationary cases, respectively, and their differences can help
289 reveal the nonstationarity of hydroclimatic responsive relationships. Accordingly, five
290 bias-correction schemes are proposed as listed in Table 1. In every scheme, 80% and
291 20% of data series are exacted for calibration and verification, respectively.
292

293 Table 1. Five bias-correction schemes.

Abbreviation	Sample pre-processing	Sample selection
SOR	Original samples (X, y): Day-to-day climatic conditions and runoff simulation (X), and runoff observation (y)	Random sampling: randomly extract 4/5 of (X, y) data series for calibration, and the remaining 1/5 for verification
SOC	Original samples	Chronological sampling: extract the first 4/5 of (X, y) data series for calibration, and the remaining 1/5 for verification
SSR	Sorted samples: Sort X by simulated runoff magnitudes (from low to high), and also for y by observed magnitudes	Random sampling
SSC	Sorted samples	Chronological sampling
SUC	Not correct biases	

294

295 (5) Uncertainty of Predictor Combinations

296 Various combinations of predictors (X) (especially climatic conditions) are
297 available for any hydrologic-model bias-correction practice. The variation is related to
298 bias-correction accuracies although the relation may be weaker than that from other
299 uncertainties (e.g., hydrologic models and bias-correction schemes) (Muleta &
300 Nicklow, 2005). In this study, the variation mainly represents the associations of
301 runoff-simulation biases with antecedent climatic conditions of different lag times.
302 Specifically, five lag times between streamflow and climatic conditions are selected as
303 listed in Table 2. In addition to simulated runoffs, four climatic variables, i.e., daily
304 accumulative precipitation (P), daily highest temperature (HT), daily lowest
305 temperature (LT), and daily mean moisture (M), at any lag time are used as predictors
306 in bias-correction modeling based on data availabilities. Cross-comparisons of
307 modeling results under these predictor combinations can differentiate the
308 contributions of incorporating antecedent climatic conditions at different lag times to

309 correcting biases of hydrologic models. This would be helpful for facilitating the
 310 other related BCHS practices.
 311

312 Table 2. Five combinations of predictors in hydro-modeling bias correction.

Abbreviation	Lag time	Selected predictors
C5x	No	R; P, HT, LT, M
C9x14	14 days	R; P, HT, LT, M; P ₁₄ , HT ₁₄ , LT ₁₄ , M ₁₄
C9x1	1 day	R; P, HT, LT, M; P ₁ , HT ₁ , LT ₁ , M ₁
C9x2	2 days	R; P, HT, LT, M; P ₂ , HT ₂ , LT ₂ , M ₂
C13x	Consecutive 2 days	R; P, HT, LT, M; P ₁ , HT ₁ , LT ₁ , M ₁ ; P ₂ , HT ₂ , LT ₂ , M ₂

313 Note: daily accumulative precipitation (P), daily highest temperature (HT), daily lowest
 314 temperature (LT), daily mean relative humidity (M), and simulated runoff (R). Subscripts
 315 represent the numbers of lag days between streamflow and antecedent climatic conditions.
 316

317 (6) Uncertainty of Hydro-Modeling Performance Indicators

318 For any hydrologic or bias-correction model, its accuracy can be represented as
 319 various indicators. For instance, correlation coefficients reflect the matchiness of
 320 simulation and observation in overall linear/nonlinear trends, error indices for the
 321 deviations of simulation with observation, while others for the similarity between
 322 them. Any indicator can hardly be suitable for assessing model accuracies from the
 323 perspective of all application practices of diverse emphases (Tian & Xu, 2015). To
 324 address such an uncertainty, eleven commonly-used indicators are employed to
 325 quantify the multi-aspect accuracies of hydrologic modeling and the associated bias
 326 correction. The abbreviations, full names, formulas, optimal values, and value ranges
 327 of these indicators are specified in Table 3.
 328

329 Table 3. Indicators of modeling accuracies.

Abbreviation	Name	Formula	Perfect/ Interval
PR	Pearson correlation coefficient	$\frac{n \sum_{i=1}^n x_i y_i - \sum_{i=1}^n x_i \sum_{i=1}^n y_i}{\sqrt{n \sum_{i=1}^n x_i^2 - (\sum_{i=1}^n x_i)^2} \sqrt{n \sum_{i=1}^n y_i^2 - (\sum_{i=1}^n y_i)^2}}$	1/-1~1
KR	Kendall correlation coefficient	$\frac{2 \sum_{i<j} \text{sgn}(x_i - x_j) \text{sgn}(y_i - y_j)}{n(n-1)}$	1/-1~1
SR	Spearman correlation coefficient	$1 - \frac{6 \sum_{i=1}^n d_i^2}{n(n^2 - 1)}$	1/-1~1

MAE	Mean absolute error	$\frac{\sum_{i=1}^n y_i - x_i }{n}$	0/0~+∞
RMSE	Root mean squared error	$\sqrt{\frac{\sum_{i=1}^n (x_i - y_i)^2}{n}}$	0/0~+∞
NRE1	Type-1 normalized root mean squared error	$\frac{\sum_{i=1}^n (x_i - y_i)^2}{\sum_{i=1}^n y_i^2}$	0/0~+∞
NRE2	Type-2 normalized root mean squared error	$\frac{RMSE}{\bar{y}}$	0/0~+∞
RAE	Relative absolute error	$\frac{\sum_{i=1}^n x_i - y_i }{\sum_{i=1}^n y_i - \bar{y} }$	0/0~+∞
RRSE	Root relative squared error	$\sqrt{\frac{\sum_{i=1}^n (x_i - y_i)^2}{\sum_{i=1}^n (y_i - \bar{y})^2}}$	0/0~+∞
NSE	Nash-Sutcliffe coefficient	$1 - \frac{\sum_{i=1}^n (x_i - y_i)^2}{\sum_{i=1}^n (y_i - \bar{y})^2}$	1/-∞~1
IOA	Similarity coefficient	$1 - \frac{\sum_{i=1}^n (x_i - y_i)^2}{\sum_{i=1}^n (x_i - \bar{x} + y_i - \bar{y})^2}$	1/-∞~1

330 Note (taking daily modeling as an example): day $i = 1, 2, 3, \dots, n$ (n is the total number of
331 samples); x_i : simulated discharge at the i^{th} day; y_i : observed discharge at the i^{th} day; \bar{x} : the average
332 of x_i ; \bar{y} = the average of y_i ; $d_i = \text{rg}(x_i) - \text{rg}(y_i)$ where $\text{rg}()$ is the rank of x_i or y_i for all i .
333

334 (7) Non-Method Uncertainties

335 There are also some other uncertainties (or multiplicities) in bias-corrected
336 hydrologic simulation from the perspective of model applications (Ajami et al., 2007;
337 Liu & Gupta, 2007b). For example, the findings of hydroclimatic relationships or

338 modeling practices for one watershed may not be transferable for another. Model
339 users may be interested in low, medium, high, or other magnitudes of streamflow,
340 depending on the discrepant, dynamic or allied importance of these magnitudes for
341 them. Daily, monthly, seasonal or yearly modeling results are required for various
342 water resources management or engineering practices (Brunner et al., 2012). To
343 address these non-method uncertainties, multiple watersheds, streamflow magnitudes,
344 and temporal scales are taken into account in this study. Specifically, (1) two
345 representative watersheds (i.e., Xiangxi and Zhongzhou) of different hydrologic,
346 climatic, geophysical, socio-economic, eco-environmental, and other characteristics in
347 southern China are selected as study areas. The selection is helpful for examining the
348 transferability of key findings of the IBCHMUA approach among different
349 watersheds. (2) Magnitudes of streamflow discharges are refined as six quantile
350 intervals (i.e., 0 to 10%, 10 to 25%, 25 to 50%, 50 to 75%, 75 to 90%, and 90 to
351 100%) of related simulations or observations. The refining can help reveal the
352 variations of bias-corrected hydrologic simulations and their accuracies with
353 streamflow magnitudes. (3) Modeling results at three temporal scales (i.e., monthly,
354 seasonal, and yearly) are composited to facilitate cross-scale analysis of hydroclimatic
355 relationships and model performances. The relevant modeling results are summarized
356 in Section 5.

357

358 **4. Impacts of Method Uncertainties**

359 **(1) Model-Performance Indicators**

360 A total of 11 indicators are employed to quantify the bias-corrected hydro-
361 modeling accuracy during verification for every combination of hydrologic models,
362 bias-correction methods and schemes, predictor combinations, watersheds,
363 streamflow magnitudes and temporal scales under the diverse uncertainties. The
364 correlation of every pair of the indicators, and the distribution and statistics of every
365 indicator for all combinations are shown in Figure 4. One representative statistic is the
366 coefficient of variation (CV) (Brian et al., 1998) that can characterize the standardized
367 dispersion of the distribution of an indicator under the uncertainties in BCHS. It can
368 be used to reflect the impact of the uncertainties on BCHS accuracies (i.e., the
369 indicators). Meanwhile, the indicators can quantify the impacts of climatic conditions
370 on the trends, absolute magnitudes, relative magnitudes, or other features of runoffs,
371 in addition to indicating BCHS accuracies. Thus, a comparison of the CVs for all
372 indicators implies that the impacts of the uncertainties in BCHS on hydro-modeling
373 accuracies (i.e., on the estimations of climatic impacts on runoffs) vary with
374 performance indicators significantly and generally decrease from the relative
375 magnitudes, through the absolute magnitudes, to the trends of runoffs.

376 In addition, significant differences exist for the similarities of the indicators. For
377 instance, RAE (i.e., the relative absolute error of a bias-corrected hydrologic model) is
378 significantly different with the other indicators. This implies that the RAE of a
379 hydrologic model calibrated according to the other indicators can hardly be
380 guaranteed and vice versa. This also reflects the significant impacts of the uncertainty
381 of performance indicators on BCHS (e.g., accuracies and results). In contrast, NSE is

382 highly positively/negatively correlated with the other indicators (except RAE); the
 383 median of its absolute correlations with the others is equal to 0.91, higher than that for
 384 any others. Although NSE cannot perfectly represent all diverse performance
 385 indicators (especially RAE), it could be the most representative indicator in BCBS
 386 studies. Compared with PR, NRE2, RRSE and IOA (of which the absolute
 387 correlations with NSE are higher than 0.90), SR, KR, MAE and RMSE show
 388 relatively lower absolute correlations with NSE although the correlations are higher
 389 than 0.82 as well as that between RAE and NSE. In the following results analyses,
 390 NSE and couple of other indicators are selected to reflect the uncertainty of
 391 performance indicators.
 392



	PR	SR	KR	MAE	RMSE	NRE1	NRE2	RAE	NSE	RRSE	IOA
Median	0.920	0.930	0.790	8.90	21.11	0.030	0.140	1.080	0.800	0.440	0.940
CV	0.133	0.101	0.212	0.731	0.515	0.789	0.985	0.106	0.282	0.503	0.096

393

394 Figure 4. Distributions, correlations and statistics of bias-corrected hydro-modeling
 395 performance indicators under all uncertainties. Upper right: correlation coefficient for
 396 every pair of indicators; lower left: scatter plot for every pair of indicators; diagonal

397 line: distribution and relative variance (i.e., variance / mean) of every indicator; table
 398 at the bottom: median, and coefficient of variation ($CV = \text{standard deviation} / \text{mean}$)
 399 of the distribution of every indicator; performance indicators are defined in Table 3.

400

401 (2) Bias-Correction Methods

402 Table 4 lists the bias-corrected hydro-modeling accuracies for Xiangxi
 403 Watershed during the verification period based on two bias-correction methods and
 404 three bias-correction schemes. The accuracies under the other combinations of
 405 hydrologic models, predictor combinations, and watersheds present similar patterns.
 406 Results show that DiPMI is more effective than LM in correcting biases of hydrologic
 407 models. The advantages of DiPMI over LM are apparent for all performance
 408 indicators. In the bias-correction scheme of SOR, both DiPMI and LM have
 409 encouraging performances, e.g., NSE raised by 95.3% and 55.2%, respectively in
 410 comparison with original biased hydrologic simulations. In the SOC scheme, the
 411 improvement of modeling accuracies is less significant than SOR due to the different
 412 foci of the two schemes (i.e., SOR on multi-year streamflow distributions, while SOC
 413 on monthly streamflow timing and magnitudes). Besides, modeling accuracies are
 414 decreased after bias corrections in some combinations (bold numbers in Table 4) of
 415 performance indicators, bias-correction methods, and bias-correction schemes. For
 416 example, bias corrections enhance the overall modeling accuracies of hydrologic
 417 models (in consideration of the representativeness of NSEs), but lead to higher RAEs
 418 (i.e., the relative absolute errors) for the verification period. The cause for this might
 419 be the nonstationarity of hydro-model biases or rainfall-runoff relationships between
 420 calibration and verification periods. A bias-corrected hydrologic model built for the
 421 calibration period may over-correct model biases that differ for the calibration and
 422 verification periods, and performs worse than the original hydrologic model in the
 423 verification period. This points out the potential limitation of bias corrections for
 424 nonstationary rainfall-runoff relationships, and the necessity of applying multiple
 425 performance indicators in evaluating bias-corrected hydrologic simulations.

426

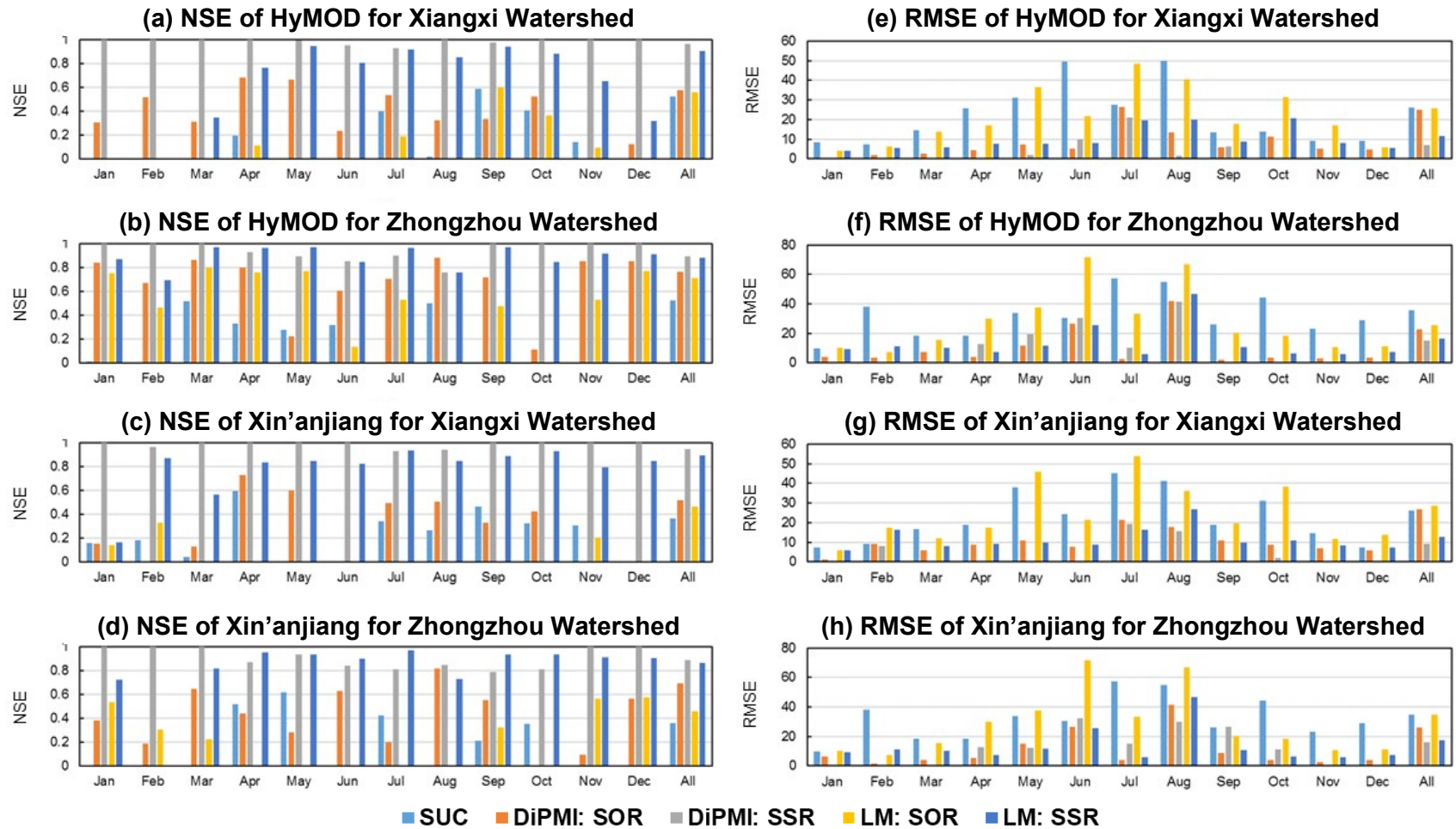
427 Table 4. Verification accuracies of hydrologic simulations through two bias-correction
 428 methods (DiPMI and LM) for Xiangxi Watershed in southern China. Performance
 429 indicators are defined in Table 3; bias-correction schemes (SUC, SOC and SOR) are
 430 defined in Table 1.

Indicators	SUC	DiPMI-SOC	DiPMI-SOR	LM-SOC	LM-SOR
KR	0.61	0.63	0.99	0.54	0.82
RMSE	26.19	25.14	6.99	25.88	11.76
RAE	1.07	1.10	1.13	1.10	1.09
NSE	0.52	0.57	0.96	0.55	0.90

431

432 The impacts of bias-correction methods (i.e., DiPMI and LM) on hydrologic
 433 simulations under combinations of watersheds, hydrologic models, temporal scales
 434 (e.g., monthly or yearly), bias-correction schemes, and performance indicators are

435 illustrated in Figure 5. Results verify the advantages of DiPMI over LM in correcting
436 biases of hydrologic models, although LM performs better than DiPMI in few cases.
437 Since performance indicators can reflect the impacts of climate change on runoffs,
438 Figure 5 shows the estimated climatic impacts on the streamflow of southern China
439 significantly vary with bias-correction methods for single months, but not for the
440 entire verification period. Namely, the impacts of the uncertainty of bias-correction
441 methods on hydrologic modeling accuracies (or the estimations of climatic impacts on
442 runoffs) increase from yearly to monthly scales. Additionally, the differences of
443 modeling accuracies between bias-correction methods are higher in the SOR scheme
444 than those in the SSR scheme. This implies the impacts of the uncertainty of bias-
445 correction methods significantly vary with bias-correction schemes (e.g., decreasing
446 from SOR to SSR). Besides, it is also shown that the impacts of the uncertainty of
447 bias-correction methods do not significantly vary with hydrologic models and present
448 significant spatial heterogeneity for different watersheds in southern China.
449



450

451 Figure 5. Verification accuracies of hydrologic models (HyMOD and Xin'anjiang) corrected by DiPMI and LM for watersheds (Xiangxi and
 452 Zhongzhou) in southern China. Performance indicators (NSE and RMSE) are defined in Table 3; bias-correction schemes (SUC, SOR and SSR)
 453 are defined in Table 1.

454 **(3) Hydrologic Models**

455 To examine the impact of the uncertainty of hydrologic models on BCHS, we
 456 analyzed the verification accuracies of two hydrologic models (i.e., HyMOD and
 457 Xin'anjiang) for the watersheds in southern China under representative scenarios of
 458 bias-correction schemes and performance-indicator selections. The relevant results are
 459 presented in Table 5. Generally, HyMOD is more capable of capturing the hydrologic
 460 processes in southern China under the impact of climate change than Xin'anjiang,
 461 which does not significantly differ for various performance indicators; its advantages
 462 over Xin'anjiang are shrunk after the biases of original hydrologic simulations being
 463 corrected. Meanwhile, HyMOD cannot outperform Xin'anjiang in all cases. For
 464 instance, both NRE2 and RRSE of the original HyMOD-based simulation of
 465 Zhongzhou Watershed are higher than those of Xin'anjiang, implying that Xin'anjiang
 466 performs better than HyMOD in simulating the relative magnitudes of runoffs in
 467 southern China under climate change. Furthermore, we may conclude that the
 468 uncertainty of hydrologic models poses significant impacts on BCHS accuracies and
 469 on the estimations of climatic impacts on runoffs in southern China, and that the
 470 significance varies with bias-correction schemes (e.g., decreasing after bias
 471 correction).

472

473 Table 5. Verification accuracies of two hydrologic models (HM and XAJ) for the
 474 watersheds (Xiangxi and Zhongzhou) in southern China under various scenarios of
 475 bias-correction schemes (SUC, SOR and SSR in Table 1) and performance-indicator
 476 selections (NSE, NRE2 and RRSE in Table 3). HM: the HyMOD hydrologic model;
 477 XAJ: the Xin'anjiang hydrologic model.

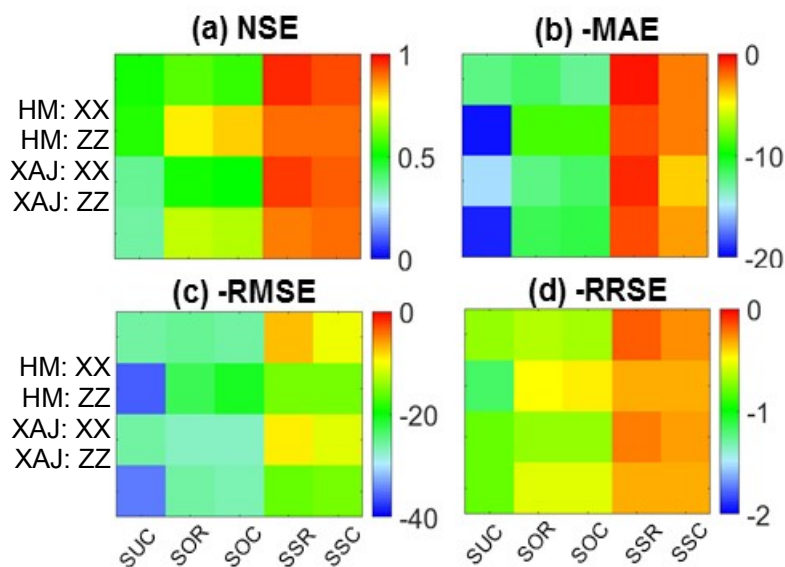
Watershed	SUC: HM			SUC: XAJ		
	NSE	NRE ₂	RRSE	NSE	NRE2	RRSE
Xiangxi	0.52	0.29	0.69	0.36	0.40	0.79
Zhongzhou	0.54	0.55	1.16	0.36	0.36	0.80
	SOR: HM			SOR: XAJ		
	NSE	NRE ₂	RRSE	NSE	NRE2	RRSE
Xiangxi	0.58	0.26	0.65	0.52	0.30	0.69
Zhongzhou	0.77	0.16	0.48	0.70	0.21	0.55
	SSR: HM			SSR: XAJ		
	NSE	NRE ₂	RRSE	NSE	NRE2	RRSE
Xiangxi	0.97	0.020	0.18	0.95	0.034	0.23
Zhongzhou	0.89	0.074	0.32	0.89	0.080	0.34

478

479 **(4) Bias-Correction Schemes**

480 In this study, five bias-correction schemes (or literally four, i.e., SOR, SOC, SSR
 481 and SSC, and the scheme of no bias correction as the baseline, i.e., SUC) are applied.
 482 Their foci differ from each other. SOR and SOC emphasize the timing of runoffs
 483 (crucial for water resources management) under the impacts of climate change, while
 484 SSR and SSC for the multi-year distribution of runoffs (especially important for
 485 relevant engineering designs). On the other hand, SOR and SSR focus on climatic
 486 impacts on runoffs in the entire historical period, while SOC and SSC on their
 487 nonstationarity (or temporal change) within the period. Comparing them with SUC
 488 can reveal the biases of original hydrologic simulations in these different aspects, and
 489 comparing all schemes can examine the impacts of the uncertainty of bias-correction
 490 schemes on hydrologic simulations.

491 Some representative results (i.e., verification accuracies of the hydrologic models
 492 corrected by the DiPMI method for the watersheds in southern China) are shown in
 493 Figure 6. They verify a few of existing findings, e.g., the significant improvement of
 494 modeling accuracies by bias correction, and the higher accuracies of hydrologic
 495 models in reproducing runoff distributions than timing. In addition, they also reveal a
 496 series of new findings. For instance, the overall impacts of climate change on multi-
 497 year distributions of runoffs are higher than those on runoff timing. The
 498 nonstationarity of rainfall-runoff relationships exists for the watersheds in southern
 499 China and poses relatively insignificant impacts on hydrologic simulations;
 500 meanwhile, it decreases from Zhongzhou to Xiangxi Watersheds, implying higher
 501 impacts of human activities on runoffs in the former watershed than the latter, and
 502 does not significantly vary with hydrologic models and performance indicators.
 503 Besides, the impacts of the uncertainty of bias-correction schemes on the accuracies
 504 of hydrologic simulations (reflecting the estimated climatic impacts on runoffs) are
 505 significant for all combinations of watersheds, hydrologic models and performance
 506 indicators, especially for Zhongzhou Watershed.
 507



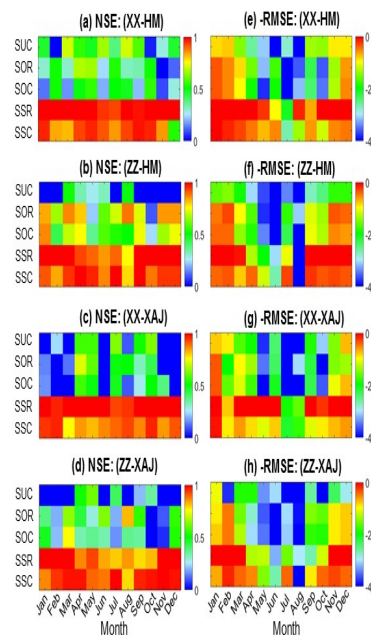
508
 509 Figure 6. Verification accuracies of hydrologic models for the watersheds in southern

510 China under various bias-correction schemes (SUC, SOR, SOC, SSR and SSC in
 511 Table 1). XX: Xiangxi Watershed; ZZ: Zhongzhou Watershed; HM: the HyMOD
 512 hydrologic model; XAJ: the Xin'anjiang hydrologic model; NSE, MAE, RMSE and
 513 RRSE: four performance indicators in Table 3.

514

515 Furthermore, the intra-annual variations of the impacts of bias-correction
 516 schemes on hydrologic simulations are presented in Figure 7. It is shown that, at the
 517 monthly scale, the impacts of bias-correction schemes on hydrologic simulations vary
 518 with performance indicators significantly. Compared with NSEs (denoting the
 519 accuracies of bias-corrected hydrologic models in reproducing the impacts of climatic
 520 conditions on both trends and magnitudes of runoffs), RMSEs (denoting those for
 521 runoff magnitudes) present V-shape patterns in the Figure. One cause for this is that
 522 the accuracies of bias-corrected hydrologic models in simulating runoff magnitudes,
 523 or the impacts of climate change on runoff magnitudes show more significant intra-
 524 annual variations than those on runoff trends. Another cause is that, in comparison
 525 with runoff magnitudes, the impacts of bias-correction schemes on the hydro-
 526 modeling accuracies for and the estimated climatic impacts on runoff trends are more
 527 significant. In addition, the intra-annual variations of the impacts of bias-correction
 528 schemes do not significantly vary with watersheds and hydrologic models; although
 529 the impacts for Xiangxi Watershed are intensified from HyMOD to Xin'anjiang, their
 530 intra-annual variations seem similar.

531



532

533 Figure 7. Verification accuracies of hydrologic models for the watersheds in southern
 534 China in every month under various bias-correction schemes (SUC, SOR, SOC, SSR

535 and SSC in Table 1). XX: Xiangxi Watershed; ZZ: Zhongzhou Watershed; HM: the
536 HyMOD hydrologic model; XAJ: the Xin'anjiang hydrologic model; NSE and
537 RMSE: two performance indicators in Table 3.

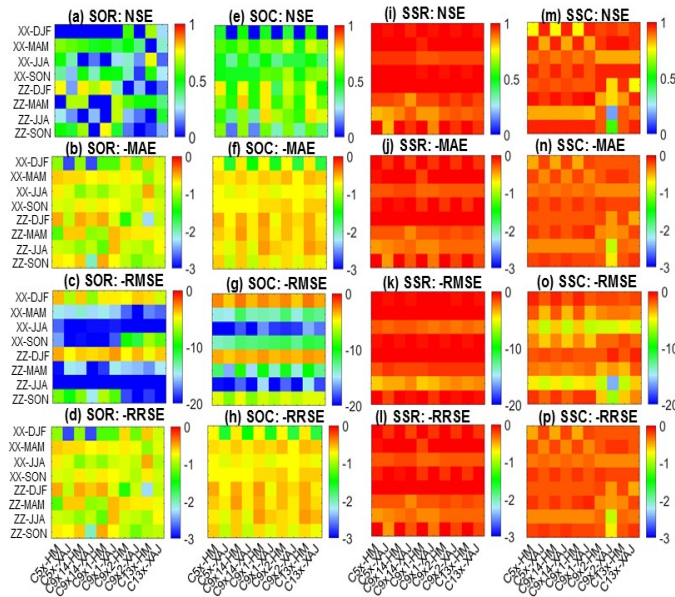
538

539 **(5) Predictor Combinations**

540 For any hydrologic simulation, multiple combinations of predictors (e.g.,
541 different climatic variables in different lag months) are optional. Such an uncertainty/
542 multiplicity may diversify hydrologic simulations (e.g., their accuracies representing
543 the impacts of climate change on runoffs) and can differentiate the impacts of various
544 predictors by comparing the simulations. Accordingly, we compared the verification
545 accuracies of bias-corrected hydrologic models for the watersheds in southern China
546 under five predictor combinations (Figure 8). The comparison is helpful for
547 investigating the impacts of the uncertainty/multiplicity of predictor combinations, as
548 well as their variations with the other uncertainties/multiplicities (e.g., hydrologic
549 models, bias-correction schemes, watersheds, performance indicators, and seasons).

550 Specifically, compared with the other uncertainties, bias-correction schemes pose
551 the most significant impacts on hydrologic simulations under various predictor
552 combinations. According to the foci of the schemes, the impacts of climate change on
553 the multi-year distributions of runoffs are significantly higher than those on runoff
554 timing regardless of the other uncertainties. Besides, the impacts of performance
555 indicators on hydrologic simulations in the bias-correction schemes of SOR and SOC
556 are more significant than those in the other two schemes. This implies that, due to the
557 nonstationarity of climatic impacts on runoffs, the impacts estimation would be more
558 sensitive with the multiplicity of performance indicators. Additionally, the impacts of
559 predictor combinations on hydrologic simulations are less significant than those of the
560 other uncertainties; according to NSEs (i.e., the most representative performance
561 indicator), they significantly vary with watersheds (decreasing from Zhongzhou to
562 Xiangxi Watersheds) and seasons (decreasing from JJA, Son, MAM to DJF) and do
563 not with hydrologic models. Meanwhile, insignificant improvements of hydrologic
564 modeling accuracies from predictor combination C5x to the others reveal that the
565 runoffs in southern China are dominated by the current-day climate under all
566 uncertainties. Generally, the impacts of predictor combinations on hydrologic
567 simulations decrease from bias-correction schemes, performance indicators, seasons,
568 watersheds to hydrologic models.

569



570

571 Figure 8. Verification accuracies of bias-corrected hydrologic models for the
 572 watersheds in southern China under various predictor combinations. Horizontal axes:
 573 predictor combinations (C5x, C9x14, C9x1, C9x2 and C13x in Table 2) and
 574 hydrologic models (HM = HyMOD and XAJ = Xin'anjiang); vertical axes:
 575 watersheds (XX = Xiangxi and ZZ = Zhongzhou) and seasons (DJF, MAM, JJA and
 576 SON); bias-correction schemes (SOR, SOC, SSR and SSC in Table 1); performance
 577 indicators (NSE, MAE, RMSE and RRSE in Table 3).

578

579 5. Impacts of Non-Method Uncertainties

580 (1) Watersheds

581 Two watersheds were selected to represent southern China. Whether and how the
 582 accuracies of hydrologic simulations vary with watersheds under all uncertainties can
 583 reflect the spatial heterogeneities of climatic impacts on runoffs in southern China,
 584 and their interactions with the other diverse uncertainties. To achieve this, analyzed all
 585 relevant modeling results. For instance, the enhancements of hydrologic modeling
 586 accuracies by bias corrections are more significant for Zhongzhou Watershed than
 587 Xiangxi Watershed (Figure 5), especially under the scenarios of HyMOD and dry
 588 seasons. Generally, the impacts of climate change on runoffs in Zhongzhou Watershed
 589 are higher than those in Xiangxi Watershed (Figure 5), implying the relatively lower
 590 impacts of non-climatic factors (e.g., water resources management or other human
 591 activities) in Zhongzhou Watershed. As shown in Table 5, the original hydrologic
 592 models underestimate the differences of climatic impacts on runoffs between the
 593 watersheds in southern China due to the existence of biases and, after bias corrections,
 594 the estimated impacts significantly vary with watersheds. Furthermore, the variation
 595 with watersheds is shrunk from the HyMOD to Xin'anjiang models (Figure 6) and is
 596 higher in the SOR and SOC schemes compared with the other bias-correction

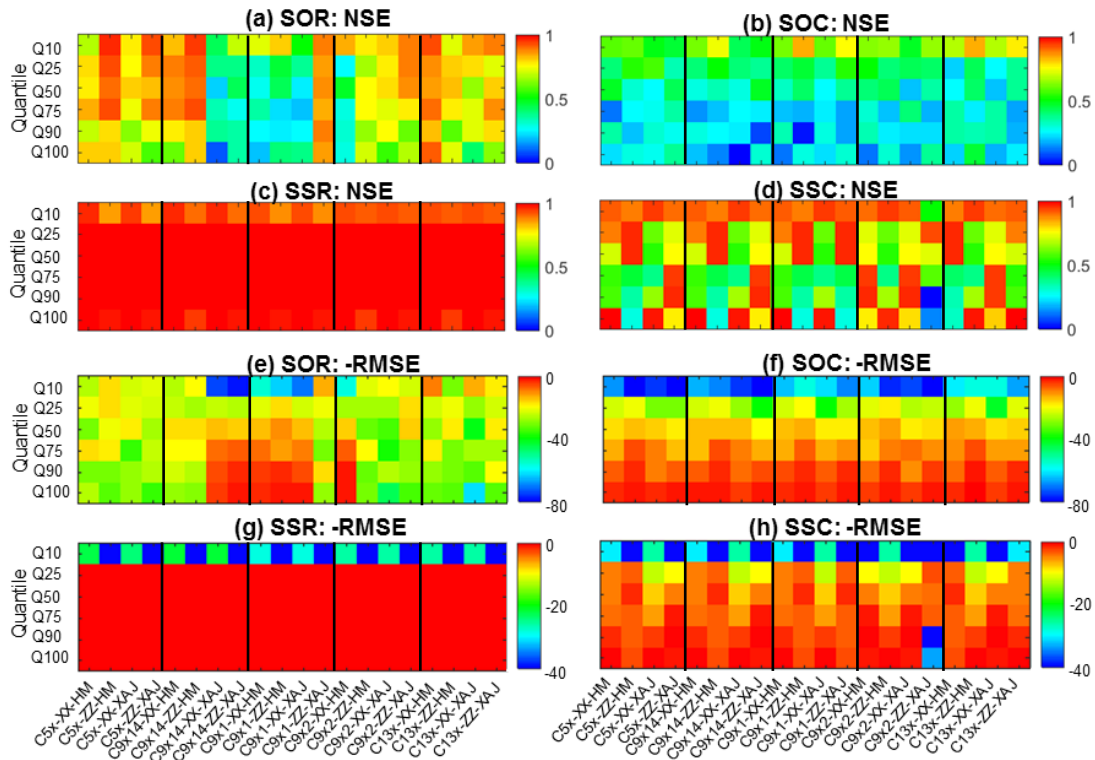
597 schemes (Figure 6 or 7). Besides, the differences of hydrologic simulations between
598 watersheds do not significantly vary with predictor selections (Figure 8).
599

600 **(2) Streamflow Magnitudes**

601 Climatic impacts on runoffs in southern China may vary with runoff magnitudes
602 (represented as quantile intervals of runoffs as defined in Section 3(7)). To reveal the
603 variational effects and their interactions with the other uncertainties, we analyzed the
604 verification accuracies of bias-corrected hydrologic models under all combinations of
605 watersheds, hydrologic models, predictor selections, runoff magnitudes, bias-
606 correction schemes, and performance indicators (Figure 9).

607 According to the bias-corrected hydrologic simulations, the overall impacts of
608 climatic conditions on runoff magnitudes and trends in southern China show
609 increasing and decreasing trends with runoff magnitudes, respectively. Namely,
610 drought trends and flood magnitudes are more sensitive with climate change
611 compared with flood trends and drought magnitudes. The impacts of climate change
612 on runoffs increase from runoff timing to distributions, their variations with
613 streamflow magnitudes show opposite trends, and the nonstationarity of rainfall-
614 runoff relationships due to human interferences would intensify these effects. The
615 variations of climatic impacts on runoffs with runoff magnitudes vary significantly
616 with predictor selections in the bias-correction scheme of SOR, while not in the other
617 schemes (i.e., SOC, SSR and SSC). This may be because the latter schemes cannot
618 eliminate anthropogenic impacts on runoffs or specify temporal variability of rainfall-
619 runoff relationships.

620 The difference of predictor combinations mainly originates the lag time (e.g., 0,
621 1, 2 or 14 lag days) between climatic conditions and runoffs. In the SOR scheme, the
622 impacts of such a difference on the variations of climatic impacts on runoffs with
623 runoff magnitudes differ for the combinations of watersheds and hydrologic models.
624 Take the impacts of climatic conditions on the runoffs of Xiangxi Watershed
625 estimated by bias-corrected HyMOD models as an example, the impacts on the lowest
626 runoffs (i.e., Q10) are the highest for the climatic conditions in the current, lag-1 and
627 lag-2 days and are the lowest for those in the current days, while the impacts on the
628 highest runoffs (Q100) are the highest for the climatic conditions in the current, lag-1
629 and lag-2 days and the lowest for those in the current and lag-1 days. Although both
630 watersheds and hydrologic models pose significant impacts on the variations of
631 rainfall-runoff relationships with runoff magnitudes, no significant patterns are found
632 for the impacts. Generally, climatic impacts on runoffs in southern China significantly
633 vary with runoff magnitudes, which further varies with bias-correction schemes,
634 performance indicators, predictor combinations, hydrologic models, and watersheds.
635



636

637

638

639

640

641

642

643

644

645

646

Figure 9. Verification accuracies of bias-corrected hydrologic models in modeling various runoff magnitudes for the watersheds in southern China. Horizontal axes: predictor combinations (C5x, C9x14, C9x1, C9x2 and C13x in Table 2), watersheds (XX = Xiangxi and ZZ = Zhongzhou), and hydrologic models (HM = HyMOD and XAJ = Xin'anjiang); vertical axes: runoff magnitudes represented as quantile intervals (i.e., Q10 = 0 to 10%, Q25 = 10 to 25%, Q50 = 25 to 50%, Q75 = 50 to 75%, Q90 = 75 to 90%, and Q100 = 90 to 100%) of runoffs; bias-correction schemes (SOR, SOC, SSR and SSC in Table 1); performance indicators (NSE and RMSE in Table 3).

647

(3) Temporal Scales

648

649

650

651

652

653

654

655

656

657

658

659

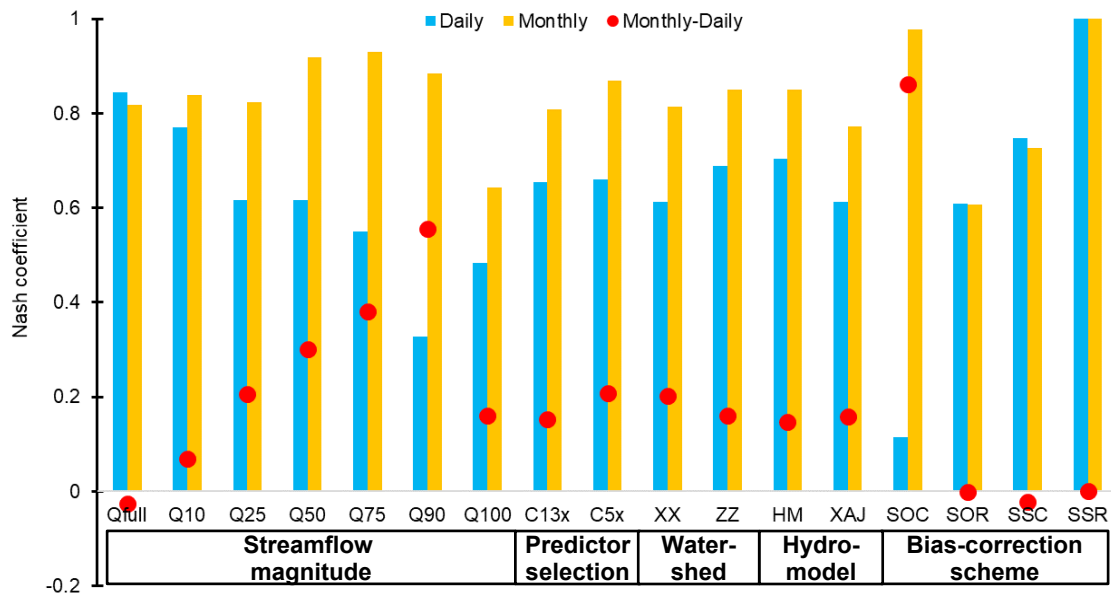
All analyses above focus on the daily-scale hydrologic simulations for southern China. To reveal the impacts of temporal scales on the simulations, as well as their interactions with every other uncertainty, we estimate the medians of the NSEs at daily and monthly scales, and their differences between both scales. Take the multiplicity/uncertainty of watersheds in southern China as an example, the median of the NSEs during the verification period for all combinations of streamflow magnitudes, predictor combinations, hydrologic models, and bias-correction schemes is calculated for every watershed (i.e., Xiangxi and Zhongzhou). The related results are presented in Figure 10. Due to the significantly low accuracies of the LM bias-correction method and the SUC bias-correction scheme as discussed above, they are excluded in the results. Only two representative predictor combinations (i.e., C13x and C5x in Table 2), and the most representative performance indicator (i.e., the NSE in Table 3) are selected.

660

661

Modeling accuracies increase from the daily to monthly scales in most cases, which has been verified in many existing studies and implies the higher impacts of

662 climatic conditions on runoffs in southern China at the monthly scale than those at the
 663 daily scale. The increments of climatic impacts on runoffs (except floods
 664 corresponding to the highest quantile interval Q100) from the daily to monthly scales
 665 show a significantly increasing trend with runoff magnitudes. This is attributable to
 666 the significant decreases in climatic impacts at the daily scale, and the insignificant
 667 difference of them at the monthly scale as runoff magnitudes increase. The difference
 668 of modeling accuracies (or the estimated climatic impacts on runoffs) between
 669 temporal scales varies with predictor combinations, watersheds, and hydrologic
 670 models, although the variation is not highly significant. In contrast, bias-correction
 671 schemes pose significant impacts on the difference that is the highest for the SOC
 672 scheme and insignificant for the others. In consideration of the differences of these
 673 schemes in characterizing runoff characteristics (e.g., timing versus distributions, and
 674 stationarity versus nonstationarity), we may conclude that the estimated nonstationary
 675 climatic impacts on runoff timing in southern China significantly vary with temporal
 676 scales. Generally, it is shown that the significance of the impacts of temporal scales on
 677 hydrologic simulations increases from hydrologic models, watersheds, predictor
 678 combinations, bias-correction schemes, to runoff magnitudes.
 679



680

681 Figure 10. Medians of the Nash coefficients of bias-corrected hydrologic simulations
 682 for the watersheds in southern China at daily and monthly scales (and their differences
 683 = Monthly-Daily). Streamflow magnitudes: Qfull (full data series), and quantile
 684 intervals (i.e., Q10 = 0 to 10%, Q25 = 10 to 25%, Q50 = 25 to 50%, Q75 = 50 to 75%,
 685 Q90 = 75 to 90%, and Q100 = 90 to 100%) of multi-year runoff observations;
 686 predictor combinations: C13x and C5x (Table 2); watersheds: XX = Xiangxi, and ZZ
 687 = Zhongzhou; hydrologic models: HM = HyMOD, and XAJ = Xin'anjiang; bias-
 688 correction schemes: SOC, SOR, SSC and SSR (Table 1).

689

690 (4) All Uncertainties

691

To reveal the interactions of the impacts of all uncertainties, we calculate the

692 medians of the NSEs (as the most representative performance indicator) for every
693 predictor combination, every hydrologic model, and every bias-correction scheme
694 under all combinations of temporal scales, watersheds, and streamflow magnitudes.
695 Due to the significantly low accuracies of the LM bias-correction method and the
696 SUC bias-correction scheme as discussed above, they are also excluded in this group
697 of results (Table 6).

698 It is shown that the modeling accuracies (or the estimated climatic impacts on
699 runoffs) increase from daily to monthly scales, and from Xiangxi to Zhongzhou
700 Watersheds. The accuracies or impacts for various runoff magnitudes are lower than
701 those for the overall runoffs for all predictor combinations, hydrologic models, and
702 most bias-correction schemes at the monthly scale, and for the SSR scheme at the
703 daily scale. As streamflow magnitudes increase, the NSEs decrease for most
704 combinations of temporal scale, watersheds, predictor combinations, hydrologic
705 models, and bias-correction schemes, although they also show nonlinear or
706 insignificant variations for the other combinations. The lag time between precipitation
707 and runoffs tends to be two days for Xiangxi Watershed and zero to one day for
708 Zhongzhou Watershed, and it varies with runoff magnitudes significantly (generally
709 decreasing with them) and temporal scales insignificantly. The HyMOD model is
710 more effective than Xin'anjiang at capturing the impacts of climate change on runoffs
711 in southern China (especially at the monthly scale, for Xiangxi Watershed, and on
712 non-flood or overall runoff magnitudes), although Xin'anjiang also shows higher
713 accuracies in a few of cases. The estimated climatic impacts on runoffs in southern
714 China are the highest for the bias-correction scheme of SSR, do not significantly vary
715 with temporal scales and watersheds for the SOR and SSR schemes, their variations
716 with the SOC and SSC schemes show opposite patterns between the daily and
717 monthly scales. Namely, the variations of the estimated climatic impacts on runoffs
718 with temporal scales, watersheds, and runoff magnitudes are significantly influenced
719 by bias-correction schemes.

720 Generally, the uncertainties in bias-corrected hydrologic simulations are
721 interactive with each other. As shown in the extension table at the bottom of Table 6,
722 the bias-corrected hydrologic modeling accuracies (or the estimated climatic impacts
723 on runoffs in southern China) increase from daily to monthly scales, from Xiangxi to
724 Zhongzhou Watersheds, from the highest through the lowest to the overall runoff
725 magnitudes, from C9x2, C9x14, C13x, C5x to C9x1 predictor combinations, from
726 Xin'anjiang to HyMOD models, and from SUC, SOC, SOR, SSC to SSR bias-
727 correction schemes. Meanwhile, the impacts of the uncertainties in bias-correction
728 hydrologic simulations decrease from bias-correction schemes, temporal scales,
729 streamflow magnitudes, hydrologic models or predictor combinations, to watersheds.
730

731 Table 6. Medians of the verification-period Nash coefficients (NSEs) for every predictor combination (i.e., C5x, C9x14, C9x1, C9x2 and C13x
732 in Table 2), every hydrologic model (i.e., HM = HyMOD and XAJ = Xin'anjiang), and every bias-correction scheme (i.e., SOC, SOR, SSC and
733 SSR in Table 1) for all combinations of temporal scales, southern-China watersheds, and streamflow magnitudes (i.e., all and quantile intervals
734 (Q10 = 0 to 10%, Q25 = 10 to 25%, Q50 = 25 to 50%, Q75 = 50 to 75%, Q90 = 75 to 90%, and Q100 = 90 to 100%) of multi-year runoff
735 observations). The maximum of the Nash coefficients for all predictor combinations, hydrologic models, or bias-correction schemes under every
736 combination of temporal scales, watersheds, and streamflow magnitudes is bolded. The extension table at the bottom lists the medians of the
737 NSEs for every alternative, and their standard deviation (SDV) for all alternatives of every uncertainty/multiplicity.

Temporal scale	Watershed	Streamflow magnitude	Predictor combination					Hydro-model		Bias-correction scheme			
			C5x	C9x1	C9x2	C13x	C9x14	HM	XAJ	SOC	SSC	SOR	SSR
Daily	Xiangxi	All	0.75	0.81	0.82	0.81	0.80	0.83	0.72	0.55	0.92	0.57	0.95
		Q10	0.72	0.68	0.73	0.77	0.75	0.77	0.73	0.37	0.83	0.57	0.88
		Q25	0.59	0.21	0.20	0.68	0.50	0.73	0.27	0.14	0.27	0.53	1.00
		Q50	0.53	0.16	0.47	0.59	0.35	0.47	0.32	0.07	0.46	0.50	1.00
		Q75	0.39	0.12	0.69	0.65	0.19	0.26	0.33	0.07	0.26	0.52	1.00
		Q90	0.27	0.17	0.70	0.60	0.27	0.28	0.26	0.07	0.28	0.31	1.00
		Q100	0.77	0.54	0.37	0.32	0.59	0.52	0.46	0.03	0.94	0.20	0.99
	Zhongzhou	All	0.85	0.84	0.59	0.78	0.84	0.85	0.71	0.62	0.90	0.67	0.93
		Q10	0.74	0.75	0.67	0.78	0.77	0.76	0.74	0.48	0.77	0.74	0.80
		Q25	0.82	0.80	0.56	0.56	0.54	0.71	0.72	0.18	0.78	0.66	1.00
		Q50	0.73	0.84	0.52	0.55	0.58	0.69	0.56	0.15	0.48	0.67	1.00
		Q75	0.82	0.04	0.43	0.42	0.47	0.12	0.65	0.03	0.12	0.65	1.00
		Q90	0.46	0.04	0.18	0.28	0.38	0.16	0.41	0.04	0.13	0.37	1.00
		Q100	0.36	0.12	0.46	0.71	0.23	0.37	0.37	0.09	0.22	0.37	0.95
Monthly	Xiangxi	All	0.70	0.75	0.78	0.81	0.74	0.78	0.76	0.39	0.92	0.43	1.00
		Q10	0.91	0.88	0.92	0.85	0.85	0.90	0.80	0.99	0.66	-0.75	1.00

	Q25	0.80	0.87	0.94	0.78	0.86	0.90	0.76	0.99	0.66	0.22	1.00
	Q50	0.93	0.94	0.89	0.91	0.93	0.92	0.90	0.99	0.68	0.63	1.00
	Q75	0.85	0.88	0.88	0.86	0.85	0.88	0.87	0.99	0.61	0.69	1.00
	Q90	0.89	0.90	0.90	0.89	0.83	0.89	0.89	0.91	0.65	0.76	1.00
	Q100	0.65	0.68	0.65	0.75	0.63	0.67	0.73	0.36	0.61	0.77	1.00
	All	0.82	0.83	0.66	0.82	0.82	0.84	0.76	0.58	0.92	0.49	1.00
	Q10	0.93	0.94	0.81	0.91	0.93	0.93	0.91	0.99	0.71	0.07	1.00
	Q25	0.90	0.90	0.84	0.86	0.92	0.90	0.89	0.99	0.75	0.32	1.00
Zhongzhou	Q50	0.96	0.93	0.87	0.89	0.90	0.92	0.88	0.99	0.78	0.63	1.00
	Q75	0.95	0.89	0.87	0.87	0.87	0.90	0.87	0.99	0.75	0.65	1.00
	Q90	0.95	0.90	0.83	0.89	0.89	0.89	0.89	0.95	0.72	0.70	1.00
	Q100	0.68	0.79	0.80	0.64	0.74	0.72	0.73	0.21	0.73	0.66	1.00
Medians of NSEs for every alternative, and their standard deviation (SDV)	Temporal scale	Daily	Monthly	SDV								
		0.56	0.87	0.22								
	Watershed	Xiangxi	Zhongzhou	SDV								
		0.74	0.77	0.02								
	Streamflow magnitude	All	Q10	Q25	Q50	Q75	Q90	Q100	SDV			
		0.81	0.78	0.77	0.76	0.72	0.71	0.64	0.05			
	Predictor combination	C5x	C9x1	C9x2	C13x	C9x14	SDV					
		0.79	0.81	0.72	0.78	0.76	0.03					
	Hydrologic model	HyMOD	Xin'anjiang	SDV								
		0.78	0.73	0.03								
Bias-correction scheme	SOC	SSC	SOR	SSR	SDV							
	0.44	0.69	0.57	1.00	0.24							

739 **6. Conclusions**

740 In this study, an integrated bias-corrected hydro-modeling uncertainty analysis
741 (i.e., IBCHMUA) approach based on DiPMI (i.e., discrete principal-monotonicity
742 inference) was developed to investigate the impacts of various uncertainties on BCHS
743 (i.e., bias-corrected hydrologic simulations). These uncertainties were classified as
744 two groups, i.e., method uncertainties (e.g., performance indicators, bias-correction
745 methods, hydrologic models, bias-correction schemes, and predictor combinations)
746 and non-method uncertainties (e.g., watersheds, streamflow magnitudes, and temporal
747 scales). The approach was applied to two representative watersheds (Xiangxi and
748 Zhongzhou) in southern China. As summarized below, a series of findings regarding
749 the impacts of these uncertainties were revealed through IBCHMUA.

750 (1) The impacts of the uncertainties in BCHS on hydro-modeling accuracies (i.e.,
751 on the estimations of climatic impacts on runoffs) vary with performance indicators
752 significantly and generally decrease from the relative magnitudes, through the
753 absolute magnitudes, to the trends of runoffs. This points out the necessity of applying
754 multiple performance indicators in evaluating BCHS. Although the Nash coefficient
755 cannot perfectly represent all diverse performance indicators, it could be the most
756 representative indicator in BCHS studies.

757 (2) DiPMI is more effective than one commonly-used method (i.e., multiple
758 linear regression) in correcting biases of hydrologic models. The impacts of the
759 uncertainty of bias-correction methods on hydro-modeling accuracies (or the
760 estimations of climatic impacts on runoffs) increase from yearly to monthly scales.
761 The impacts of the uncertainty of bias-correction methods significantly vary with
762 bias-correction schemes, do not with hydrologic models, and present significant
763 spatial heterogeneity for watersheds in southern China.

764 (3) HyMOD is more capable of capturing the hydrologic processes in southern
765 China under the impact of climate change than Xin'anjiang, and Xin'anjiang performs
766 better in simulating the relative magnitudes of runoffs. The uncertainty of hydrologic
767 models poses significant impacts on BCHS accuracies (or the estimations of climatic
768 impacts on runoffs), and the significance varies with bias-correction schemes (e.g.,
769 decreasing after bias correction). The nonstationarity of rainfall-runoff relationships
770 decreases from Zhongzhou to Xiangxi Watersheds, implying higher impacts of human
771 activities on runoffs in the former watershed than the latter, and does not significantly
772 vary with hydrologic models and performance indicators.

773 (4) The impacts of the uncertainty of bias-correction schemes on the accuracies of
774 hydrologic simulations (or the estimated climatic impacts on runoffs) are significant
775 for all combinations of watersheds, hydrologic models and performance indicators,
776 especially for Zhongzhou Watershed. At the monthly scale, the impacts of bias-
777 correction schemes on BCHS vary with performance indicators significantly. The
778 intra-annual variations of the impacts of bias-correction schemes do not significantly
779 vary with watersheds and hydrologic models. Compared with the other uncertainties,
780 bias-correction schemes pose the most significant impacts on BCHS under various
781 predictor combinations. Due to the nonstationarity of climatic impacts on runoffs, the
782 impact estimation is sensitive with the multiplicity of performance indicators.

783 (5) The impacts of predictor combinations on BCHS are less significant than
784 those of the other uncertainties, significantly vary with watersheds (decreasing from
785 Zhongzhou to Xiangxi Watersheds) and seasons (decreasing from JJA, Son, MAM to
786 DJF) and do not with hydrologic models. The runoffs in southern China are
787 dominated by the current-day climate under all uncertainties. The impacts of predictor
788 combinations on hydrologic simulations decrease from bias-correction schemes,
789 performance indicators, seasons, watersheds to hydrologic models.

790 (6) The enhancements of hydrologic modeling accuracies by bias corrections are
791 more significant for Zhongzhou Watershed than Xiangxi Watershed. The impacts of
792 climate change on runoffs in Zhongzhou Watershed are higher than those in Xiangxi
793 Watershed, implying the relatively lower impacts of non-climatic factors (e.g., water
794 resources management or other human activities) in Zhongzhou Watershed. The
795 original hydrologic models underestimate the differences of climatic impacts on
796 runoffs between the watersheds in southern China due to the existence of biases and,
797 after bias corrections, the estimated impacts significantly vary with watersheds. The
798 variation with watersheds is shrunk from the HyMOD to Xin'anjiang models and is
799 higher in the SOR and SOC schemes compared with the other bias-correction
800 schemes. The differences of hydrologic simulations between watersheds do not
801 significantly vary with predictor selections.

802 (7) The overall impacts of climatic conditions on runoff magnitudes and trends in
803 southern China show increasing and decreasing trends with runoff magnitudes,
804 respectively. The impacts of climate change on runoffs increase from runoff timing to
805 distributions, their variations with streamflow magnitudes show opposite trends, and
806 the nonstationarity of rainfall-runoff relationships due to human interferences would
807 intensify these effects. The variations of climatic impacts on runoffs with runoff
808 magnitudes vary significantly with predictor selections in the bias-correction scheme
809 of SOR, while not in the other schemes. Climatic impacts on runoffs in southern
810 China significantly vary with runoff magnitudes, which further varies with bias-
811 correction schemes, performance indicators, predictor combinations, hydrologic
812 models, and watersheds.

813 (8) The impacts of climatic conditions on runoffs in southern China at the
814 monthly scale are higher than those at the daily scale. The increments of climatic
815 impacts on runoffs (except floods) from the daily to monthly scales show a
816 significantly increasing trend with runoff magnitudes. The estimated nonstationary
817 climatic impacts on runoff timing in southern China significantly vary with temporal
818 scales. The significance of the impacts of temporal scales on BCHS increases from
819 hydrologic models, watersheds, predictor combinations, bias-correction schemes, to
820 runoff magnitudes.

821 (9) Generally, the uncertainties in BCHS are interactive with each other. The bias-
822 corrected hydrologic modeling accuracies (or the estimated climatic impacts on
823 runoffs in southern China) increase from daily to monthly scales, from Xiangxi to
824 Zhongzhou Watersheds, from the highest through the lowest to the overall runoff
825 magnitudes, from C9x2, C9x14, C13x, C5x to C9x1 predictor combinations, from
826 Xin'anjiang to HyMOD models, and from SUC, SOC, SOR, SSC to SSR bias-

827 correction schemes. Meanwhile, the impacts of the uncertainties in BCHS decrease
828 from bias-correction schemes, temporal scales, streamflow magnitudes, hydrologic
829 models or predictor combinations, to watersheds.

830 These findings are of great significance for hydrologic simulations under
831 uncertainties, as well as for water resources management practices over southern
832 China and the other similar watersheds. As one of few attempts to comprehensively
833 examine diverse uncertainties in BCHS, this study can be improved in various
834 aspects. For example, data uncertainty, spatial-scale uncertainty, and uncertainty of
835 climate models may contribute significantly to the uncertainty of hydrologic
836 simulations. An analysis of predictor interactions may help improve simulation
837 efficiencies. A systematic multifactorial analysis would help quantify both individual
838 and interactive impacts of all uncertainties in BCHS. Many subsequent studies will be
839 conducted to achieve these and some other potential improvements of this study.

840

841 **Acknowledgments**

842 This research was supported by the National Key Research and Development
843 Plan (2016YFC0502800), the Natural Sciences Foundation (51520105013,
844 51679087), the 111 Program (B14008) and the Natural Science and Engineering
845 Research Council of Canada. Data were collected and are available from Hydrological
846 Yearbook of the People's Republic of China at the National Library of China, and
847 China National Meteorological Information Center (<http://data.cma.cn/site/index.html>).

848

849 **References**

- 850 Addor, N., Rössler, O., Köplin, N., Huss, M., Weingartner, R., & Seibert, J. (2014).
851 Robust changes and sources of uncertainty in the projected hydrological regimes of
852 Swiss catchments. *Water Resources Research*, 50(10), 7541-7562.
- 853 Arkesteijn, L., & Pande, S. (2013). On hydrological model complexity, its geometrical
854 interpretations and prediction uncertainty. *Water Resources Research*, 49(10),
855 7048-7063.
- 856 Beven, K., & Binley, A. (1992). The future of distributed models: model calibration
857 and uncertainty prediction. *Hydrological processes*, 6(3), 279-298.
- 858 Beven, K., & Binley, A. (1992). The future of distributed models: model calibration
859 and uncertainty prediction. *Hydrological processes*, 6(3), 279-298.
- 860 Buizza, R., Houtekamer, P. L., Pellerin, G., Toth, Z., Zhu, Y., & Wei, M. (2005). A
861 comparison of the ECMWF, MSC, and NCEP global ensemble prediction systems.
862 *Monthly Weather Review*, 133(5), 1076-1097.
- 863 Chen, J., Brissette, F. P., Chaumont, D., & Braun, M. (2013). Finding appropriate bias
864 correction methods in downscaling precipitation for hydrologic impact studies over
865 North America. *Water Resources Research*, 49(7), 4187-4205.
- 866 Cheng, G. H., Huang, G. H., Dong, C., Baetz, B. W., & Li, Y. P. (2017). Interval
867 Recourse Linear Programming for Resources and Environmental Systems
868 Management under Uncertainty. *Journal of Environmental Informatics*, 30(2).
- 869 Cheng, G., Dong, C., Huang, G., Baetz, B. W., & Han, J. (2016a). Discrete principal-
870 monotonicity inference for hydro-system analysis under irregular nonlinearities,

871 data uncertainties, and multivariate dependencies. Part I: methodology
872 development. *Hydrological Processes*, 30(23), 4255-4272.

873 Cheng, G., Dong, C., Huang, G., Baetz, B. W., & Han, J. (2016b). Discrete principal-
874 monotonicity inference for hydro-system analysis under irregular nonlinearities,
875 data uncertainties, and multivariate dependencies. Part II: Applied to streamflow
876 simulation in the Xingshan Watershed. *Hydrological Processes*, 30(23), 4273-4291.

877 Cheng, G., Huang, G., Dong, C., Zhou, X., Zhu, J., & Xu, Y. (2017). Climate
878 classification through recursive multivariate statistical inferences: a case study of
879 the Athabasca River Basin, Canada. *International Journal of Climatology*, 37,
880 1001–1012.

881 Cheng, G., Huang, G., Dong, C., Zhu, J., Zhou, X., & Yao, Y. (2017). High-resolution
882 projections of 21st century climate over the Athabasca River Basin through an
883 integrated evaluation-classification-downscaling-based climate projection
884 framework. *Journal of Geophysical Research*, 122(5), 2595–2615.

885 Ehret, U., Zehe, E., Wulfmeyer, V., Warrach-Sagi, K., & Liebert, J. (2012). HESS
886 Opinions" Should we apply bias correction to global and regional climate model
887 data?". *Hydrology and Earth System Sciences*, 16(9), 3391-3404.

888 Evaristo, J., Jasechko, S., & McDonnell, J. J. (2015). Global separation of plant
889 transpiration from groundwater and streamflow. *Nature*, 525(7567), 91-94.

890 Everitt, Brian (1998). *The Cambridge Dictionary of Statistics*. Cambridge, UK New
891 York: Cambridge University Press. ISBN 978-0521593465.

892 Gupta, H. V, Kling, H., Yilmaz, K. K., & Martinez, G. F. (2009). Decomposition of
893 the mean squared error and NSE performance criteria: Implications for improving
894 hydrological modelling. *Journal of Hydrology*, 377(1–2), 80–91.

895 Haerter, J. O., Hagemann, S., Moseley, C., & Piani, C. (2010). Climate model bias
896 correction and the role of timescales. *Hydrology and Earth System Sciences
897 Discussions*, 7(5), 7863-7898.

898 Holliday, C. R., & Thompson, A. H. (1979). Climatological characteristics of rapidly
899 intensifying typhoons. *Monthly Weather Review*, 107(8), 1022-1034.

900 Krause, P., Boyle, D. P., & Båse, F. (2005). Comparison of different efficiency criteria
901 for hydrological model assessment. *Advances in geosciences*, 5, 89-97.

902 LaValle, S. M., Branicky, M. S., & Lindemann, S. R. (2004). On the relationship
903 between classical grid search and probabilistic roadmaps. *The International Journal
904 of Robotics Research*, 23(7-8), 673-692.

905 Lenderink, G., Buishand, A., & Deursen, W. V. (2007). Estimates of future discharges
906 of the river Rhine using two scenario methodologies: direct versus delta approach.
907 *Hydrology and Earth System Sciences*, 11(3), 1145-1159.

908 Liu, W., Zhan, J., Wang, C., Li, S., & Zhang, F. (2018). Environmentally sensitive
909 productivity growth of industrial sectors in the Pearl River Delta. *Resources,
910 Conservation and Recycling*, 139, 50-63.

911 McBean, E., Huang, G., Yang, A., Cheng, H., Wu, Y., Liu, Z., ... & Bhatti, M. (2019).
912 The effectiveness of exfiltration technology to support sponge city objectives.
913 *Water*, 11(4), 723.

914 Muleta, M. K., & Nicklow, J. W. (2005). Sensitivity and uncertainty analysis coupled

915 with automatic calibration for a distributed watershed model. *Journal of hydrology*,
916 306(1-4), 127-145.

917 Piani, C., Weedon, G. P., Best, M., Gomes, S. M., Viterbo, P., Hagemann, S., &
918 Haerter, J. O. (2010). Statistical bias correction of global simulated daily
919 precipitation and temperature for the application of hydrological models. *Journal of*
920 *hydrology*, 395(3-4), 199-215.

921 Saber, M., & Yilmaz, K. K. (2018). Evaluation and bias correction of satellite-based
922 rainfall estimates for modelling flash floods over the Mediterranean region:
923 application to Karpuz River Basin, Turkey. *Water*, 10(5), 657.

924 Shrestha, M., Acharya, S. C., & Shrestha, P. K. (2017). Bias correction of climate
925 models for hydrological modelling—are simple methods still useful?.
926 *Meteorological Applications*, 24(3), 531-539.

927 Tian, Y., Xu, Y. P., Booij, M. J., & Wang, G. (2015). Uncertainty in future high flows
928 in Qiantang River Basin, China. *Journal of hydrometeorology*, 16(1), 363-380.

929 Tu, M. C., & Smith, P. (2018). Modeling pollutant buildup and washoff parameters
930 for SWMM based on land use in a semiarid urban watershed. *Water, Air, & Soil*
931 *Pollution*, 229(4), 1-15.

932 Vetter, T., Reinhardt, J., Flörke, M., van Griensven, A., Hattermann, F., Huang, S., ...
933 & Krysanova, V. (2017). Evaluation of sources of uncertainty in projected
934 hydrological changes under climate change in 12 large-scale river basins. *Climatic*
935 *Change*, 141(3), 419-433.

936 Wi, S., Yang, Y. C. E., Steinschneider, S., Khalil, A., & Brown, C. M. (2015).
937 Calibration approaches for distributed hydrologic models in poorly gaged basins:
938 implication for streamflow projections under climate change. *Hydrology and Earth*
939 *System Sciences*, 19(2), 857-876.

940 Wilby, R. L., & Harris, I. (2006). A framework for assessing uncertainties in climate
941 change impacts: Low-flow scenarios for the River Thames, UK. *Water resources*
942 *research*, 42(2).

943 Ye, A., Duan, Q., Yuan, X., Wood, E. F., & Schaake, J. (2014). Hydrologic post-
944 processing of MOPEX streamflow simulations. *Journal of hydrology*, 508, 147-
945 156.

946 Yin, Z., Liao, W., Lei, X., Wang, H., & Wang, R. (2018). Comparing the Hydrological
947 Responses of Conceptual and Process-Based Models with Varying Rain Gauge
948 Density and Distribution. *Sustainability*, 10(9), 3209.

949 Yuan, F., Ren, L. L., Yu, Z. B., & Xu, J. (2008). Computation of potential
950 evapotranspiration using a two-source method for the Xin'anjiang hydrological
951 model. *Journal of Hydrologic Engineering*, 13(5), 305-316.

952 Zhang, X., Dong, Z., Gupta, H., Wu, G., & Li, D. (2016). Impact of the Three Gorges
953 Dam on the hydrology and ecology of the Yangtze River. *Water*, 8(12), 590.